Applied Catalysis B: Environmental 95 (2010) 87–92

Contents lists available at ScienceDirect

Applied Catalysis B: Environmental

journal homepage: www.elsevier.com/locate/apcatb

Steam reforming of methanol over ceria and gold-ceria nanoshapes

Nan Yi, Rui Si, Howard Saltsburg, Maria Flytzani-Stephanopoulos *

Department of Chemical and Biological Engineering, Tufts University, Medford, MA 02155, USA

ARTICLE INFO

Article history:
Received 2 October 2009
Received in revised form 8 December 2009
Accepted 9 December 2009
Available online 16 December 2009

Keywords:
Gold
Cerium oxide nanoparticles
Steam reforming of methanol
Water–gas shift reaction
Methanol decomposition
Shape effect

ABSTRACT

In this work we have found that a small amount (~1 at.%) of gold deposited on ceria nanorods exhibits excellent catalytic activity for the low-temperature steam reforming of methanol (SRM). Gold clusters (<1 nm, TEM invisible) dispersed on the {1 1 0} faces of ceria nanorods catalyze the reaction in a cooperative mechanism with ceria. Gold nanoparticles (~3 nm) on the {1 0 0} surfaces of ceria nanocubes are inactive. The apparent activation energy of the SRM reaction on Au-ceria is ~110 kJ mol^{-1}. On the basis of TPSR/MS analysis, we determined that the SRM reaction on Au-ceria involves methanol dehydrogenation, methyl formate hydrolysis and formic acid decomposition steps to produce CO_2 and H_2. Better than 97% catalyst selectivity to CO_2 was found over the temperature range from 175 to 250 °C. In the presence of methanol, the water–gas shift (WGS) reaction is suppressed and is not part of the mechanism at temperatures below 250 °C. The SRM stability of the Au-ceria system is good for practical application of this type catalyst.

1. Introduction

Clean and efficient hydrogen production is of interest because hydrogen is envisioned as the fuel of the future. Methanol is a good source of hydrogen because of its high hydrogen/carbon ratio, safe handling, and easy synthesis from renewable and fossil fuels. Methanol can be used to produce hydrogen via the following three processes: decomposition, steam reforming, and partial oxidation. Methanol decomposition is endothermic, gives a high CO yield, and is therefore, unsuitable for PEM fuel cell application. Partial oxidation of methanol is an exothermic reaction with a rapid start-up and a dynamic response. Nevertheless, the formation of hot spots in the reactor may result in catalyst sintering, and carbon deposition; it also produces a diluted hydrogen stream by the nitrogen in the air. Steam reforming of methanol (SRM), an endothermic reaction, has the highest yield of H_2, and depending on the catalyst used, the selectivity to CO_2 can be very high. Thus it can be used to generate H_2 on demand for small-scale PEM fuel cells [1].

Steam reforming of methanol should be carried out at low-temperature to exploit the favorable thermodynamics to yield low CO. Most of the previous investigations have focused on Cu-Zn based catalysts because of the extensive use of such catalysts for methanol synthesis [2,3]. To address some obvious drawbacks with Cu-based catalysts including deactivation, pyrophoricity, and high-temperature sintering, addition of a third component (Al, Zr or Ce) has been tried [4–6] to increase the dispersion of copper as well as the surface area. Efforts to replace Cu-based catalysts [7,8] have included selective formulations from the Group VIII metals, especially, Pd–Zn alloys, which show high activity and excellent CO_2 selectivity.

To date, few reports exist on the catalytic applications of gold supported on oxides for methanol conversion reactions. Bowker et al. [9] found that Au/TiO_2 can photocatalyze the reforming of methanol in aqueous solutions. Chang et al. [10] reported that Au/TiO_2 catalysts show relatively high activity in partial oxidation of methanol, and correlated the activity with the particle size of metallic gold. Previous work by our group has investigated the activity of nanoscale ceria, suitably modified with small amounts of gold, for the low-temperature water–gas shift (WGS) reaction [11–15]. The active catalyst involves atomically dispersed gold in ceria, Au-O-Ce. The most active state is the fully oxidized surface. As shown by Deng et al. [14], formation of gold clusters in a hydrogen-rich atmosphere begins the process of deactivation, i.e. the loss of Au-O-Ce active sites. A strong correlation between the ceria shape and the WGS activity of Au-ceria was recently reported by Si and Flytzani-Stephanopoulos [13]. Since the WGS reaction is often included in the reaction mechanism of steam reforming of methanol, it is of interest to investigate whether Au-ceria is active for the SRM and whether the decomposition of methanol followed by water–gas shift is the pathway of SRM over Au-ceria catalysts.

In this work, we have examined the Au-ceria system as an SRM catalyst, and investigated the dependence of the activity and selectivity of the methanol reaction on the crystal morphology of

* Corresponding author at: 4 Colby Street, Medford, MA 02155, USA. Tel.: +1 617 627 3048; fax: +1 617 627 3991.
E-mail address: maria.flytzani-stephanopoulos@tufts.edu (M. Flytzani-Stephanopoulos).

0926-3373/$ – see front matter © 2009 Elsevier B.V. All rights reserved.
doi:10.1016/j.apcatb.2009.12.012

ceria using suitably synthesized nanoshapes (rods and cubes) of ceria onto which gold was deposited in a second step.

2. Experimental

2.1. Catalyst preparation

Gold-ceria was synthesized in a two-step process previously reported [13]. Different shapes of nanoscale ceria (nanorods and nanocubes) were prepared via a controlled hydrolysis method using $Ce(NO_3)_3{\cdot}6H_2O$ as the precursor and NaOH as the base, followed by a hydrothermal treatment in an autoclave. The combination of different concentrations of base (C_{NaOH}) and different temperature (T) and time used in the autoclave, controls the crystal growth of CeO_2 to desired shapes and sizes. The applied values of C_{NaOH} and T were varied according to the target crystal shape: (1) rod: C_{NaOH} = 6 mol/L, T = 100 °C; (2) cube: C_{NaOH} = 6 mol/L, T = 180 °C. Calcination (2 °C min^{-1} to 400 °C, air, 4 h) of the ceria single crystals took place before applying gold onto their surfaces. Deposition–precipitation (DP) at pH 9 (base: $(NH_4)_2CO_3$) was used to deposit gold hydroxide onto the ceria surfaces from an aq. solution of $HAuCl_4$ [15].

2.2. Characterization

The BET surface area was determined by single-point N_2 adsorption/desorption cycles in a Micromeritics AutoChemII 2920. High resolution transmission electron microscopy (HRTEM) was performed using a JEOL 2010 at 200 kV. The TEM samples were prepared by drying an ethanol suspension containing dispersed catalyst powders on carbon film-coated copper grids. The average ceria particle size was estimated from *ca.* 100 nanoparticles in the images. Temperature programmed oxidation (TPO) of used catalysts was carried out to check for potential carbon deposition using a heating rate of 5 °C min^{-1} from 30 to 750 °C in 20% O_2/He with a flow rate of 70 mL min^{-1}. The outlet gas was analyzed using an on-line residual gas analyzer (MKS model RS-1).

2.3. Catalytic tests

The temperature programmed reaction studies and steady-state catalytic SRM tests were carried out in a fixed-bed quartz microreactor (6 mm OD, 4 mm ID) at atmospheric pressure. Typically 60 mg (for temperature programmed studies) and 100 mg (for catalytic reactions) of catalysts in powder form were loaded in the quartz tube. The catalysts were diluted with quartz powder at a weight ratio of 1/3. Samples were pre-reduced at 300 °C in 20% H_2/He flowing at 70 mL min^{-1}. For CH_3OH-TPSR, the reduced sample was exposed to 16 mol% methanol vapor in He flowing at 70 mL min^{-1} for 30 min at room temperature. Then, the temperature was increased linearly at 5 °C min^{-1} in the same gas mixture. For ($CH_3OH + H_2O$)-TPSR, a gas mixture of methanol and water was generated by flowing pure helium at RT through a bubbler filled with methanol and water. For the steady-state reaction tests, a pre-mixed solution of methanol and water was injected into a He gas stream by a syringe pump and vaporized in the heated gas line before entering the reactor. The feed gas comprised a mixture of CH_3OH/H_2O/He with a molar ratio of 2/2.6/95.4 and a total gas flow rate of 70 mL min^{-1}, giving a gas hourly space velocity (GHSV) of 42,000 h^{-1} at NTP. The feed and product gas streams were analyzed on-line by a residual gas analyzer (MKS model RS-1).

3. Results and discussion

3.1. Sample characterization

The properties of the Au-ceria nanoshapes and those of the gold-free ceria nanoshapes are shown in Table 1. The BET specific surface areas of the ceria nanocrystals were essentially unchanged after gold addition. We also calculated the specific surface areas using the average particle sizes and the geometric shapes of ceria from the TEM images [13]. The ceria nanorods give *ca.* 27 $m^2\ g^{-1}$ for each of the {1 1 0} and {1 0 0} surfaces, and the same value was calculated for the {1 0 0} surfaces of the ceria nanocubes. As shown in Table 1, the experimental BET values are 105 $m^2\ g^{-1}$ for nanorod (~52 $m^2\ g^{-1}$ for each of the {1 1 0} and {1 0 0} surfaces, i.e. close to twice the calculated numbers), and 27 $m^2\ g^{-1}$ for the nanocubes, i.e. the same as the calculated value. No gold particles were observed by TEM on the ceria nanorods, while on average 3 nm gold particles were found on the {1 0 0} faces of the ceria nanocubes. Combined with XPS results reported in [13], it is clear that ceria nanorods stabilize positively charged gold ions and clusters on the {1 1 0} surfaces. This explains why these surfaces have high activity for the WGS reaction, while the gold nanoparticles on the {1 0 0} surfaces are inactive [11,13]. It is noteworthy that the original shape of the catalysts is preserved after the WGS reaction, and after steam reforming of methanol, as shown in Fig. 1(a) and (b) for the SRM-used catalysts. Again, gold particles (*ca.* 3 nm) only were found on the ceria nanocubes; while gold atoms and clusters not visible by TEM were present on the ceria nanorods.

3.2. Activity evaluation

Methanol conversion was studied as a function of temperature over the 1% Au-ceria and undoped ceria samples, by ramping up the temperature as shown in Fig. 2(a). Steady-state data were collected by keeping each temperature constant for 1.5 h. Reduction of the samples with 20% H_2/He at 300 °C, preceded the activity tests. Addition of gold improved the activity of the undoped ceria dramatically. The 1% Au-ceria (rod) catalyst showed full methanol conversion at ~300 °C, and no hysteresis or deactivation was observed upon cooling to lower temperatures, Fig. 2(a). The same was also the case for the 1% Au-ceria (cube) catalyst. However, the latter was much less active than the former, which is attributed to the state of gold on its {1 0 0} surfaces, as will

Table 1
Physical properties and SRM activity of ceria and Au-ceria nanoshapes.

Sample	S_{BET} ($m^2\ g_{cat}^{-1}$)	Au dispersion (%)[a]	E_a (kJ mol^{-1})[b]	Rate ($\mu mol\ g_{cat}^{-1}\ s^{-1}$)[c]
Ceria (nanorods)	105 (54)[d]	–	136 ± 2.7	4.3
Ceria (nanocubes)	27 (27)[d]	–	168 ± 2.3	1.2
1% Au-ceria (rod)	100	100[e]	110 ± 0.9	12.3
1% Au-ceria (cube)	24	30	110 ± 1.2	0.2

[a] The dispersion of gold was estimated from the particle size (avg. 100 particles) in the TEM images.
[b] Apparent activation energy of steam reforming of methanol (SRM).
[c] Rate measured at 400 °C for ceria and at 250 °C for Au-ceria; gas composition: 2% CH_3OH/2.6% H_2O/95.4% He.
[d] Specific surface areas in parentheses were calculated based on the nanoparticle size and shape.
[e] Dispersion of sub-nm particles (HRTEM-invisible) set at 100%.

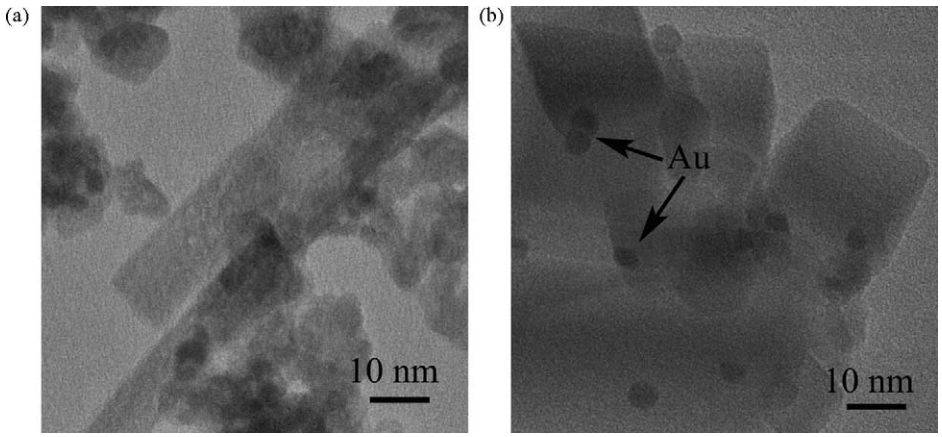

Fig. 1. HRTEM images of SRM-used Au-ceria samples (a) 1% Au-ceria (rod) and (b) 1% Au-ceria (cube).

be discussed below. This difference is not due to the small difference (2×) of the specific surface area of the two ceria nanoshapes, see Table 1, but due to the intrinsic activity difference of the metallic gold nanoparticles (present on the {1 0 0} surfaces of the ceria nanocubes) and the small gold clusters (<1 nm, present in the {1 1 0} surfaces of the ceria nanorods). After three cycles, including heating to 300 °C in the reaction gas mixture, cooling to room temperature in He, and reheating to 300 °C in the reaction gas mixture, the Au-ceria (rod) sample retained its fresh-state activity. Hence, the SRM stability of Au-ceria is promising for potential practical application.

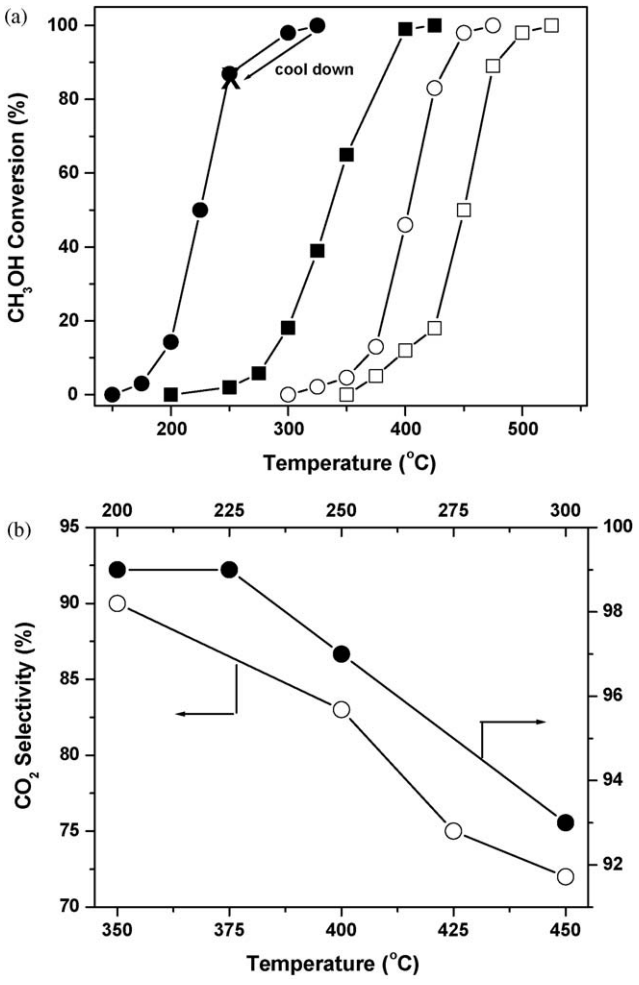

Fig. 2. (a) CH_3OH conversion (%) in steady-state tests of steam reforming of methanol over nanoshapes of CeO_2 and Au-CeO_2; ramp up temperature tests 1% Au-ceria (rod) (●); 1% Au-ceria (cube) (■);ceria (rod) (○); ceria (cube) (□); 1% Au-ceria (rod) after cooling down to 250 °C (X); gas composition: 2% CH_3OH/2.6% H_2O/bal.He; GSHV = 42,000 h^{-1}; (b) CO_2 selectivity (%) in steady-state light off tests of steam reforming of methanol over nanoshapes of ceria (rod) (○) and 1% Au-ceria (rod) (●). Gas composition: 2% CH_3OH/2.6% H_2O/bal.He; GHSV = 42,000 h^{-1}.

The CO_2 selectivity of 1% Au-ceria (rod) is shown in Fig. 2(b). This material has high CO_2 selectivity (>93%) over the whole range of temperatures tested. In the temperature range 175–250 °C, the CO_2 selectivity exceeds 97%. The same was true also for the 1% Au-ceria (cube)—data not shown. The CO_2 selectivity measured here is higher than the equilibrium CO_2 selectivity, which indicates that the water–gas shift reaction is not involved in the pathway of steam reforming of methanol, as is the case for the PdZn alloy catalyst [16]. However, over the undoped ceria crystals, the CO_2 selectivity dropped with increasing methanol conversion. This is shown in Fig. 2(b) for the ceria nanorods. Over the undoped ceria, methanol decomposition to CO and H_2 followed by the water–gas shift reaction is inferred from our data. Decomposition of methanol to CO + H_2 has been found in surface studies of methanol decomposition over thin-film ceria [17].

The steady-state SRM reaction rates were measured under differential reactor conditions, and the apparent activation energies were calculated. While the rates were much lower on the 1% Au-ceria (cube) than on the 1% Au-ceria (rod), the apparent activation energies were the same, ~110 kJ mol^{-1}, Table 1. Since the samples were reduced at 300 °C prior to reaction, all the gold was reduced, but in the case of the gold on the ceria nanorods, the size of the gold clusters remained <1 nm, as they were invisible by HRTEM. After leaching the calcined parent sample using NaCN solution as detailed in [13], the 1% Au-ceria (cube) had very little (~0.03% by ICP) residual gold. The SRM activity of this leached sample was the same as that of the parent sample. Hence, the 3 nm gold nanoparticles are not active for the SRM reaction, and in the 1% Au-ceria (cube) all the catalysis is done by the interaction of the residual gold and ceria. The number of these active sites is very few compared to the 1% Au-ceria (rod). This can explain the difference in the corresponding reaction rates shown in Table 1. Because the amount of interacting gold with ceria is so small on the cube surfaces, we cannot convert these values to turnover rates. However, all evidence (same activation energies and CO_2 selectivities, and same reaction intermediates), as will be discussed below, point to a structure–insensitive SRM reaction on Au-ceria. In other words, gold clusters (not particles) coupled with the O-Ce sites catalyze the reaction on both the {1 0 0} and {1 1 0} ceria surfaces by the same reaction pathway.

The apparent activation energy of SRM over Au-ceria catalysts is close to values obtained on $Cu/ZnO/Al_2O_3$ catalysts, 105 kJ mol^{-1}

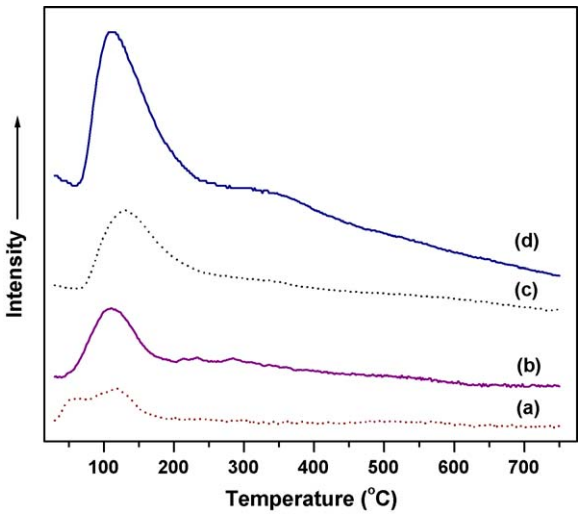

Fig. 3. TPO Profiles over fresh and used (after SRM; gas condition: 2% CH_3OH/2.6% H_2O/bal.He, 15 h-on-stream, up to 300 °C) 1% Au-ceria (rod). (a) CO_2 from fresh sample; (b) CO_2 from used sample; (c) H_2O from fresh sample and (d) H_2O from used sample.

[18]. Much higher E_{app} values were found for the undoped ceria nanocubes, 168 ± 2.3 kJ mol^{-1}, and ceria nanorods, 136 ± 2.7 kJ mol^{-1} (Table 1). It is known that the methanol decomposition reaction on ceria is structure-sensitive [19]. Potentially the two different values we found here are indicative of a similar structure sensitivity of the SRM reaction on ceria {1 0 0} and {1 1 0} surfaces.

TPO tests were carried out on the fresh and used catalysts to investigate the catalyst stability in the SRM reaction. Only adventitious carbon from atmospheric exposure was found on both the fresh and used samples. Decomposition of carbonates and desorption of water show peaks centered at ~120 °C, Fig. 3. No higher-temperature carbonate formation or carbon deposition took place. This corroborates the cyclic catalyst stability in heating–cooling tests discussed above, and further shows that the SRM stability of the Au-ceria system is good for practical application of this type catalyst.

3.3. Temperature programmed surface reaction

Temperature programmed surface reaction (TPSR) was used to study the interaction between the reactant and catalyst surface. In CH_3OH-TPSR over the 1% Au-ceria (rod), hydrogen was formed starting at ~175 °C (Fig. 4(a), Temp. I). Carbon dioxide and methane were also detected in the outlet gas, products of the decomposition of methyl formate [20,21].

$$HCOOCH_3 \rightarrow CO_2 + CH_4$$

At the same time, a small amount of methyl formate and formic acid was observed in the effluent gas along with the hydrogen, as shown in the inset of Fig. 4(a). This indicates that decomposition of methanol follows the methyl formate pathway [20,21],

$$2CH_3OH \rightarrow HCOOCH_3 + 2H_2$$

The formation of formic acid can be attributed to the conversion of dioxymethylene, H_2COO,

$$2H_2COO_{(a)} \rightarrow 2HCOO_{(a)} + H_{2(g)}$$

The short-lived species, dioxymethylene, was also reported on ceria thin films [17] and the undoped ceria investigated in this work (data not shown) to explain the formation of formic acid species.

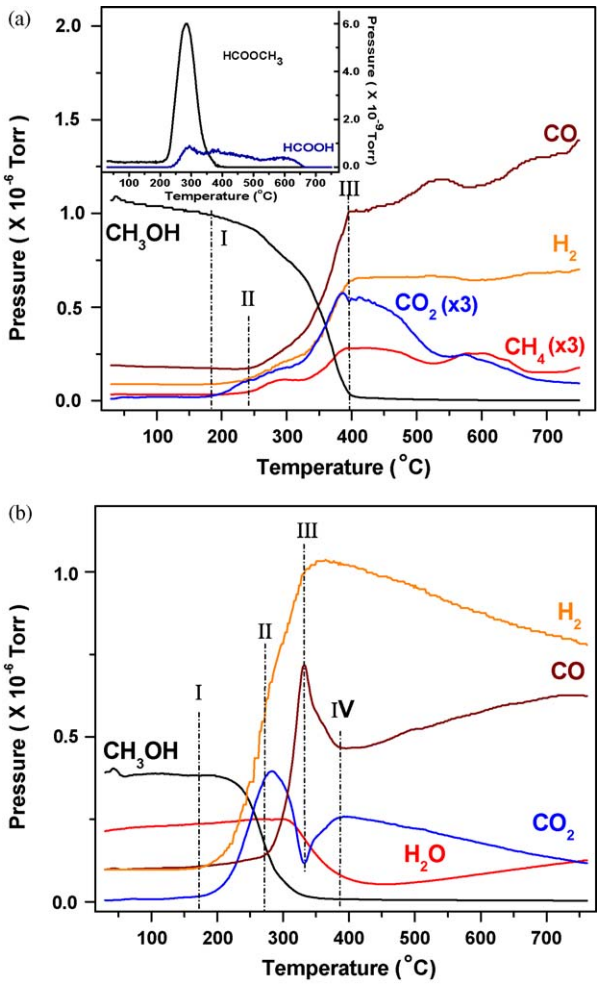

Fig. 4. (a) CH_3OH-TPSR and (b) (CH_3OH + H_2O)-TPSR profiles over 1% Au-ceria (rod).

The temperature for CO formation was higher than that for the other species. Hence, CO may derive from the decomposition of methyl formate, but it competes with the formation of CO_2 and CH_4 [20–23]. Another possibility is that CO may derive from the reverse water–gas shift reaction, from the CO_2 and H_2 formed.

To explore the role of water in methanol decomposition, (CH_3OH + H_2O)-TPSR was carried out for the two Au-ceria catalysts under investigation. In (CH_3OH + H_2O)-TPSR over 1% Au-ceria (rod), hydrogen and carbon dioxide were formed at temperatures as low as 175 °C (Fig. 4(b), Temp. I). This agrees with the activity test results that showed that hydrogen and carbon dioxide were produced in this temperature region, Fig. 2(a).

Carbon monoxide was observed starting at ~250 °C (Temp. II in Fig. 4(b)). In the temperature range from 275 to 335 °C the formation of CO may be due to decomposition of methoxy on ceria as described in Scheme 1 below. Another possibility is that reverse water–gas shift occurs. Either scheme would account for the corresponding drop in CO_2 selectivity. In the range between III (335 °C) and IV (395 °C), the concentration of CO and water decreases sharply while CO_2 and H_2 increase. As methanol conversion is complete at 325 °C, less methoxy is adsorbed and hence much more CO is able to adsorb on the gold active site, and the water–gas shift reaction takes place. This suggests that the presence of methanol inhibits the water–gas shift reaction.

At temperatures above IV (395 °C), the reverse water–gas shift reaction dominates. Finally, the lack of methyl formate species and

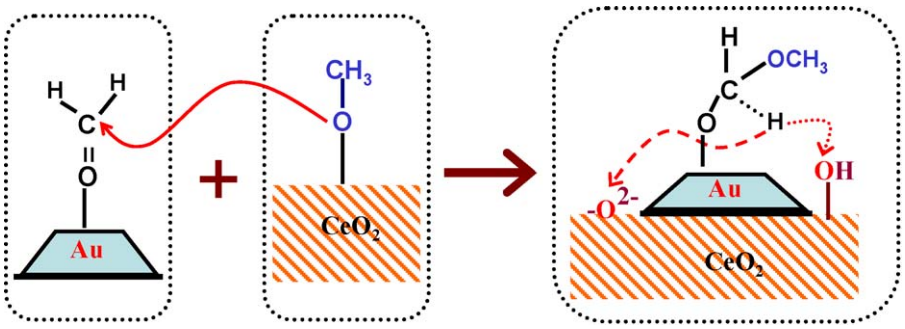

Scheme 1. Proposed cooperative reaction scheme for the steam reforming of methanol over Au-ceria. The active gold structure is a cluster of gold atoms of sub-nm size.

only trace amounts of methane in ($CH_3OH + H_2O$)-TPSR, suggests that methyl formate hydrolysis took place,

$$HCOOCH_3 + H_2O \rightarrow HCOOH + CH_3OH$$

Indeed, trace amounts of formic acid were detected in the effluent gas in this temperature region.

3.4. Mechanistic considerations

The mechanism of steam reforming of methanol is still being debated even for well-studied systems. For example, on the Pd–Zn alloy catalyst, the methyl formate route has been suggested [8]. At the same time, the methanol decomposition—water–gas shift reaction pathway has been claimed by some groups for Cu-based catalysts [24,25]; while others report the methyl formate route for copper catalysts [18,22]. Furthermore, according to the literature [26,27], formaldehyde will form after methanol is adsorbed on IB group metals (Cu, Ag and Au) because the intermediate methoxy (CH_3O) species is stabilized on those metal surfaces. Compared with Pt and Pd, Au (1 1 0), (1 1 1) facilitates the formation of methyl formate [26,27]. This can explain the different product distribution between Group VIII and Group IB metal-doped ceria in the methanol decomposition reaction [28].

In order to further investigate the mechanism of steam reforming of methanol over Au-ceria, carbon monoxide was added to the feed mixture of methanol and water. Two different concentrations of carbon monoxide (5% and 20% by volume) were introduced into the reaction system at 225 °C. It was found that the production rates of hydrogen and the ratio of H_2/CO_2 did not change. When carbon monoxide was added into the mixture, the concentration of H_2O did not change, and the conversion of methanol remained the same, as shown in Fig. 5. This further suggests that the water–gas shift reaction is not involved in the SRM reaction pathway [18] on gold catalysts.

On the basis of these findings, we propose the following SRM reaction pathway on Au-ceria:

$$2CH_3OH \rightarrow HCOOCH_3 + 2H_2 \quad (I)$$

$$HCOOCH_3 + H_2O \rightarrow HCOOH + CH_3OH \quad (II)$$

$$HCOOH \rightarrow CO_2 + H_2 \quad (III)$$

We also measured the rates and compared the activation energies for the decomposition of methanol, and compared them to those reported here for steam reforming of methanol over the Au-ceria catalysts. We found similar apparent reaction activation energies [28], and similar intermediate products, suggesting that the rate limiting step in the two reactions is the same. Both reactions share the methyl formate route, and the SRM reaction pathway does not involve the water–gas shift reaction.

The role of ceria in Au-ceria catalysts deserves special mention. Higher surface area ceria with higher oxygen storage capacity has been suggested to prevent carbon coking in the decomposition of methanol [29]. Previous work by our group has shown that ceria plays an important role in stabilizing gold clusters and controlling the gold oxidation state. It was found that cerium oxide with the highest surface area and highest number of surface oxygen species retains the highest amount of gold [12,30]. A strong crystal plane effect of ceria on the Au-ceria activity has been identified in the WGS reaction [13]. Thus, ceria nanorods facilitate the dispersion of gold on their {1 1 0} surfaces; while gold could not be dispersed on the {1 0 0} surfaces. As a result, the 1% Au-ceria (cube) material was not active for the WGS reaction [13].

For the methanol steam reforming reaction, it appears that gold clusters (<1 nm) and ceria produce methyl formate in a cooperative way, involving the surface oxygen of ceria close to the gold clusters, as shown in Scheme 1. The methoxy group is stabilized on reduced ceria [17], and the formation of methyl formate has been proposed on gold, assisted by atomic oxygen [26]. From the present work, we find that gold nanoparticles (3 nm avg. size) on the ceria nanocubes are too big to get activated by the ceria surface oxygen sites. This is why removal of the gold nanoparticles by NaCN leaching, does not reduce the activity of the Au-ceria nanocubes, containing now just ~0.03% Au, probably fully dispersed and stabilized on the ceria (1 0 0) surfaces. Thus, the reaction mechanism is concluded to involve Au and O-Ce sites on the {1 1 0} or the {1 0 0} ceria surfaces.

It has been found that methanol adsorbs weakly and molecularly on a clean gold surfaces [26,31]. However, on oxygen-covered gold (1 1 1) surfaces, the formation of small gold clusters [27] takes place and on these, stronger adsorption of methanol [26,27,31] has been reported. In the present work, ceria can provide the active oxygen to the small gold clusters stabilized

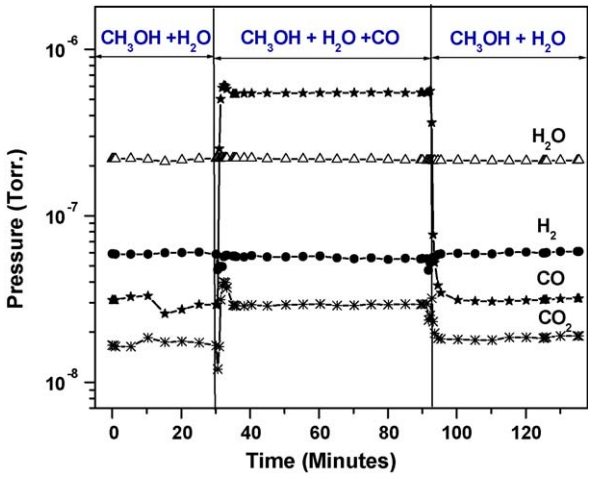

Fig. 5. Effect of the addition/removal of carbon monoxide in the reaction gas mixture over 1% Au-ceria (rod) operating at steady-state SRM at 225 °C; GHSV = 42,000 h^{-1}.

on its surface. The different crystal planes of ceria have different energetics towards oxygen vacancy formation, the {1 1 0} being the most favorable [32,33]. We compared the methanol conversion over pre-reduced Au-Ceria with pre-oxidized samples (data not shown), and found that the pre-reduced samples showed much higher activity in SRM [28]. This corroborates the argument that gold clusters stabilized at surface oxygen vacancies of ceria are the active sites for SRM. Kundakovic et al. [34] have reported that the interaction between water and ceria strongly depends on the presence of reduced cerium, Ce^{3+}, and Rh facilitates the adsorption of water on ceria. Water and hydrogen desorbed as products following water adsorption on the reduced ceria surface compared with weakly adsorbed water on the oxidized ceria.

Based on previous studies [26,35] formaldehyde is stable on gold surfaces and can then easily continue to react with methoxy or other sources of oxygen to form methyl formate or formate groups. However this path leads to CO_2 and H_2O instead of CO_2 and H_2. As we find here that methyl formate and hydrogen appear together and H_2 and CO_2 are the dominant species, we can rule out the decomposition of formate on gold.

In summary, we suggest a cooperative mechanism for Au-ceria in steam reforming of methanol as depicted by Scheme 1: reduced ceria adsorbs methanol as methoxy which combines with the formaldehyde adsorbed on gold. The methyl formate pathway is then followed. Adsorbed water helps to hydrolyse methyl formate to formic acid, as in the above set of reactions (reactions (I)–(III)).

It should be pointed out that the 1% Au-ceria (rod) catalyst shows excellent activity for the water–gas shift reaction, comparable to Au-ceria nanopowders, including Au-rhodia ceria with a high surface area of 250 $m^2\ g^{-1}$, while the Au-ceria (cube) is inactive [13]. The question then arises why the Au-ceria (rod) catalyst does not show any WGS activity at temperatures below 250 °C, at the conditions of Figs. 4 and 5. This can only be explained if a competitive adsorption exists between CO and methanol [36,37], the latter being more strongly adsorbed on the gold clusters. Based on literature reports [38,39], methanol has a higher heat of adsorption on Au (1 1 1) than CO. We have begun to look at this interesting property. In a separate experiment, it was found that addition of methanol into a steady-state water–gas shift reaction condition changed the product gas distribution [28]. More detailed investigations are planned for the future.

4. Conclusions

We have investigated gold on nanoscale ceria as a new active and stable catalyst for the methanol steam reforming reaction. Fully dispersed gold on the {1 1 0} surfaces of ceria nanorods; and gold nanoparticles (3 nm size) on ceria {1 0 0} nanocubes were compared. Only sub-nm gold clusters in the proximity of ceria oxygen species are active for the SRM reaction. From TPSR/MS and steady-state kinetics measurements, we propose that methanol steam reforming on Au-ceria proceeds through a cooperative mechanism involving oxygen from methoxy adsorbed on ceria and formaldehyde adsorbed on gold to produce methyl formate, which is then hydrolysed to formic acid, from which carbon dioxide and hydrogen are produced. This explains the better than 97% selectivity to CO_2 at all temperatures up to 250 °C. These high CO_2 selectivities are possible because the water–gas shift is not part of the SRM reaction pathway. Further proof of this is that addition of CO during steady-state SRM tests at 225 °C did not alter the reaction products. Apparently, methanol is the preferred adsorbate over CO on gold clusters. With its high activity, low propensity to CO formation, and stability over the temperature range we investigated, Au-ceria emerges as a very promising catalyst for practical applications of low-temperature steam reforming of methanol.

Acknowledgments

The financial support of this work by the U.S. DOE/BES-Hydrogen Fuel Initiative Program (#DE-FG02-05ER15730) is gratefully acknowledged. The authors thank Micromeritics for generously supplying the Autochem II 2920 as part of their Instrument Grant Program. Y.N. also thanks Y. Zhai and B. Zugic for their help with some of the experiments; and Prof. Liuye Mo and M. Boucher for helpful discussions.

References

[1] D.R. Palo, R.A. Dagle, J.D. Holladay, Chem. Rev. 107 (2007) 3992.
[2] P.L. Hansen, J.B. Wagner, S. Helveg, J.R. Rostrup-Nielsen, B.S. Clausen, H. Topsøe, Science 295 (2002) 2053.
[3] K. Klier, Appl. Surf. Sci. 19 (1984) 267.
[4] W. Dow, W.Y. Wang, T. Huang, J. Catal. 184 (1999) 357.
[5] Y.F. Li, X.F. Dong, W.M. Lin, Int. J. Hydrogen Energy 29 (2004) 1617.
[6] S. Patel, K.K. Pant, J. Power Sources 159 (2006) 139.
[7] N. Iwasa, S. Masuda, N. Ogawa, N. Takezawa, Appl. Catal. A 125 (1995) 145.
[8] N. Iwasa, N. Takezawa, Top. Catal. 22 (2003) 215.
[9] M. Bowker, L. Millard, J. Greaves, D. James, J. Soares, Gold Bull. 37 (2004) 170.
[10] F.W. Chang, H.Y. Yu, L.S. Roselin, H.C. Yang, Appl. Catal. A 290 (2005) 138.
[11] Q. Fu, H. Saltsburg, M. Flytzani-Stephanopoulos, Science 301 (2003) 935.
[12] Q. Fu, W. Deng, H. Saltsburg, M. Flytzani-Stephanopoulos, Appl. Catal. B 56 (2005) 57.
[13] R. Si, M. Flytzani-Stehphanopoulos, Angew. Chem. Int. Ed. 47 (2008) 2884.
[14] W. Deng, A.I. Frenkel, R. Si, M. Flytzani-Stephanopoulos, J. Phys. Chem. C 112 (2008) 12834.
[15] Q. Fu, A. Weber, M. Flytzani-Stephanopoulos, Catal. Lett. 77 (2001) 87.
[16] R.A. Dagle, A. Platon, D.R. Palo, A.K. Datye, J.M. Vohs, Y. Wang, Appl. Catal. A 342 (2008) 63.
[17] D.R. Mullins, M.D. Robbins, J. Zhou, Surf. Sci. 600 (2006) 1547.
[18] C.J. Jiang, D.L. Trimm, M.S. Wainwright, N.W. Cant, Appl. Catal. A 97 (1993) 145.
[19] R.M. Ferrizz, G.S. Wong, T. Egami, J.M. Vohs, Langmuir 17 (2001) 2464.
[20] R.O. Idem, N.N. Bakhshi, Ind. Eng. Chem. Res. 33 (1994) 2056.
[21] A. Gazsi, T. Bánsági, F. Solymosi, Catal. Lett. 131 (2009) 33.
[22] K. Takahashi, N. Takezawa, H. Kobayashi, Appl. Catal. 2 (1982) 363.
[23] K. Takahashi, H. Kobayashi, B. Takezawa, Chem. Lett. (1985) 759.
[24] E. Santacesaria, S. Carrà, Appl. Catal. 5 (1983) 345.
[25] B.A. Peppley, J.C. Amphlett, L.M. Kearns, R.F. Mann, Appl. Catal. A 179 (1999) 31.
[26] D.A. Outka, R.J. Madix, J. Am. Chem. Soc. 109 (1987) 1708.
[27] B.J. Xu, X.Y. Liu, J. Haubrich, R.J. Madix, C.M. Friend, Angew. Chem. Int. Ed. 48 (2009) 4206.
[28] N. Yi, Ph.D. Dissertation, Tufts University, in progress.
[29] N. Laosiripojana, S. Assabumrungrat, Chem. Eng. Sci. 61 (2006) 2540.
[30] Q. Fu, Ph.D. Dissertation, Tufts University, Febuary 2004.
[31] J.L. Gong, D.W. Flaherty, R.A. Ojifinni, J.M. White, C.B. Mullins, J. Phys. Chem. C 112 (2008) 5501.
[32] A. Trovarelli, Catal. Rev. Sci. Eng. 38 (1996) 439.
[33] M. Nolan, S.C. Parker, G.W. Watson, Phys. Chem. Chem. Phys. 8 (2006) 216.
[34] L. Kundakovic, D.R. Mullins, S.H. Overbury, Sur. Sci. 457 (2000) 51.
[35] D.A. Outka, R.J. Madix, Surf. Sci. 179 (1987) 361.
[36] C.J. Jiang, D.L. Trimm, M.S. Wainwright, N.W. Cant, Appl. Catal. A 93 (1993) 245.
[37] J.P. Breen, F.C. Meunier, J.R.H. Ross, Chem. Commun. (1999) 2247.
[38] G. Mcelhiney, J. Pritchard, Surf. Sci. 60 (1976) 397.
[39] W.K. Chen, S.H. Liu, M.J. Cao, Q.G. Yan, C.H. Lu, J. Mol. Struct. (Theochem.) 770 (2006) 87.